

Cosmic Neutrinos and their Detection

C. Haggmann

*Lawrence Livermore National Laboratory
7000 East Avenue, Livermore, CA 94550*

The standard Big-Bang theory predicts a cosmic neutrino background with an average number density of $\sim 100/\text{cm}^3$ per flavor. The most promising way of its detection is measuring the feeble “neutrino wind” forces exerted on macroscopic targets. The expected acceleration is $\sim 10^{-23}\text{cm/s}^2$ for Dirac neutrinos with a local number density $\sim 10^7/\text{cm}^3$. A novel torsion balance design is presented, which addresses the sensitivity-limiting factors of existing balances, such as seismic and thermal noise, and angular readout resolution and stability.

I. INTRODUCTION

According to the standard Big Bang model, a cosmic neutrino background, similar to the familiar microwave background, should exist in our universe. Because of their weak interactions, cosmic neutrinos fell out of thermal equilibrium at $t \simeq 1$ sec, and have been redshifting since then. Neutrinos of mass $\ll 10^{-3}$ eV would still be relativistic today, have a Fermi-Dirac spectrum with $T \simeq 1.9$ K, and be spatially uniform with $n_{\nu_L} = n_{\bar{\nu}_R} \simeq 50/\text{cm}^3$ per flavor. In contrast, neutrinos of mass $\gg 10^{-3}$ eV would be nonrelativistic today, and be clustered around galaxies with a typical velocity $v_\nu \simeq 10^{-3}$. They contribute to the cosmological energy density an amount $\Omega_\nu \simeq \sum_i m_{\nu_i}/(92h^2\text{eV})$, where $h \simeq 0.65$ is the Hubble expansion rate in units of $100\text{ km s}^{-1}\text{Mpc}^{-1}$, and where the sum includes all neutrino flavors that are nonrelativistic today. Massive neutrinos are a natural candidate for the hot component in currently favored “Mixed Hot+Cold Dark Matter (HCDM)” [1] models of galaxy formation. In this scenario, neutrinos would contribute $\simeq 20\%$ ($\sum_i m_{\nu_i} \simeq 8$ eV), and CDM (*e.g.* Wimps and axions) the remainder of the dark matter. Another popular model involving a cosmological constant is Λ HCDM [2] with $\Omega_\nu \simeq 0.05 - 0.1$. The available phase space for massive neutrinos [3,4] restricts the local neutrino number density to

$$n_\nu < 2 \times 10^6 \text{ cm}^{-3} \left(\frac{v_m}{10^{-3}} \right)^3 \sum_i \left(\frac{m_{\nu_i}}{10 \text{ eV}} \right)^3. \quad (1)$$

where v_m is the maximum neutrino velocity in the halo. Hence, neutrinos of $m_\nu \sim \text{eV}$, cannot account for all of the local halo matter density $\sim 300\text{ MeV}/\text{cm}^3$.

The detection of cosmic neutrinos by interactions with single electrons or nucleons is unlikely because of the extremely small rates and energy deposits. Past proposals have therefore focused on detecting the coherent mechanical effects on macroscopic targets due to the “neutrino wind”. In 1974, Stodolsky [5] suggested to use the energy splitting of an electron,

$$\Delta E = \sqrt{2} G_F v_e ((n_{\nu_e} - n_{\bar{\nu}_e}) - (n_{\nu_\mu} - n_{\bar{\nu}_\mu}) - (n_{\nu_\tau} - n_{\bar{\nu}_\tau})) \quad (2)$$

moving through the neutrino background with velocity v_e . However even for large neutrino number asymmetries, *e.g.* $n_{\bar{\nu}_e} = 0$, $n_{\nu_{\mu,\tau}} = n_{\bar{\nu}_{\mu,\tau}}$, $\Delta E \sim 1.3 \times 10^{-33}\text{eV}(v_e/10^{-3})(n_{\nu_e}/10^7\text{cm}^{-3})$ is still tiny. In principle, this effect could be measured by observing a torque on a permanent magnet, which is shielded against magnetic noise with superconductors. A benefit of this detection method is that it works equally well for Dirac and Majorana neutrinos. Other forces $\propto G_F$ arising from the reflection or refraction of neutrinos by macroscopic objects have been proposed by several authors [6–8]. However, all of these ideas were later found to be flawed [9,10].

Another approach is to consider forces $\propto G_F^2$ due to random elastic neutrino scattering [11–14]. Here, spatial coherence dramatically increases the cross section of targets smaller than the neutrino wavelength λ_ν . In the nonrelativistic limit, one must distinguish between Majorana and Dirac neutrinos. For Dirac μ or τ neutrinos, the cross section is dominated by the vector neutral current contribution

$$\sigma_D \simeq \frac{G_F^2 m_\nu^2}{8\pi} N_n^2 = 2 \times 10^{-55} \left(\frac{m_\nu}{10 \text{ eV}} \right)^2 N_n^2 \text{ cm}^2 \quad (3)$$

where N_n is the number of neutrons in the target of size $< \lambda_\nu/2\pi = 20 \mu\text{m} (10 \text{ eV}/m_\nu)(10^{-3}/v_\nu)$. For Majorana neutrinos the vector contribution to the cross section is suppressed by a factor $(v_\nu/c)^2$ and potentially the largest contribution arises from the axial current. The cross section of a spin-polarized target is $\sigma_M \propto N_s^2$, where N_s is the number of aligned spins in the grain.

Due to the Sun's peculiar motion ($v_s \sim 220 \text{ km/s}$) through the galaxy, a test body will experience a neutrino wind force through random neutrino scattering events. The wind direction is modulated with the sidereal period of 23hrs+56min due to the combined effects of the Earth's diurnal rotation and annual revolution around the Sun. For Dirac neutrinos, the acceleration of a target of density ρ and optimal radius $\lambda_\nu/2\pi$ has an amplitude [11,12]

$$a = 8 \times 10^{-24} \left(\frac{A-Z}{A} \right)^2 \left(\frac{v_s}{10^{-3}} \right)^2 \left(\frac{n_\nu}{10^7 \text{ cm}^{-3}} \right) \left(\frac{\rho}{20 \text{ gcm}^{-3}} \right) \frac{\text{cm}}{\text{s}^2} \quad (4)$$

and is independent of m_ν . For clustered Majorana neutrinos, the acceleration is suppressed by a factor $\sim 10^6 (10^3)$ for an unpolarized (polarized) target. For unclustered relativistic neutrinos, the force should be aligned with the direction of the microwave background dipole. Neutrinos of Dirac or Majorana type would have the same cross section, giving rise to an acceleration $\sim 10^{-34} \text{ cm/s}^2$. A target size much larger than λ_ν can be assembled, while avoiding destructive interference, by using foam-like [11] or laminated materials [12]. Alternatively, grains of size $\sim \lambda_\nu$ could be randomly embedded (with spacing $\sim \lambda_\nu$) in a low density host material.

II. DETECTOR CONCEPT

The measurement of the neutrino-induced forces and torques will require major improvements in sensor technology. At present, the most sensitive detector of small forces is the ‘‘Cavendish-type’’ torsion balance (see Figure 1), which has been widely used for measurements of the gravitational constant and searches for new forces. A typical arrangement consists of a dumbbell shaped test mass suspended by a tungsten fiber inside a vacuum chamber at room temperature. The angular deflection is usually read out with an optical lever. The torsional oscillation frequency is constrained by the yield strength of the fiber to $> 1 \text{ mHz}$. Internal friction in the fiber limits the Q to $< 10^6$. Nonlinearities in the suspension make the balance quite sensitive to seismic noise. Additional background forces arise from thermal noise and time varying gravity gradients due to tides, weather, traffic, people etc. The angular resolution of optical levers is $\sim 10^{-10} \text{ rad}$ and the smallest measurable acceleration is $\sim 10^{-13} \text{ cm/s}^2$ [15].

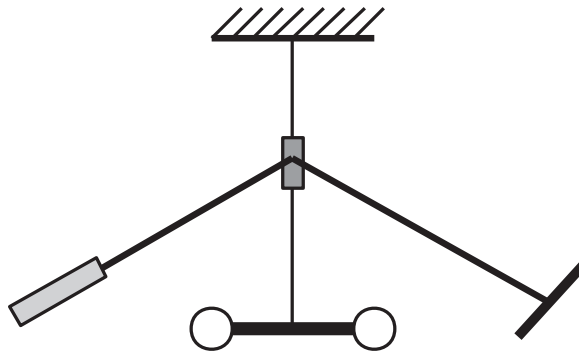


FIG. 1. Schematic diagram of a ‘‘Cavendish’’ torsion balance, which has been widely used in experimental gravity.

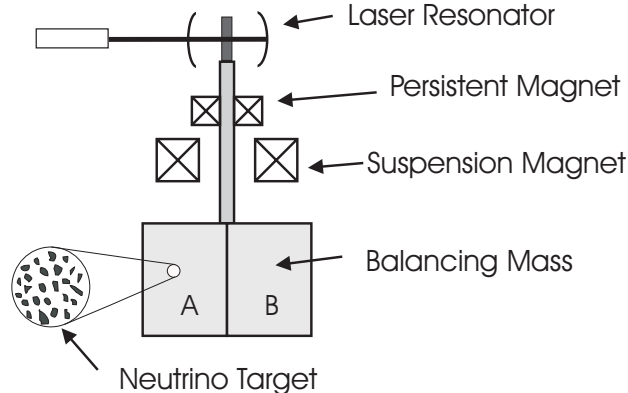


FIG. 2. Schematic diagram of the torsion oscillator. The target consists of two hemicylindrical masses with similar densities but different neutrino cross section. The target of mass \sim kg is suspended by a “magnetic hook” consisting of a superconducting magnet in persistent mode floating above a stationary magnet. The rotation angle is read out with a tunable optical cavity and an ultra-stable laser.

Several improvements seem possible (see Figure 2): Thermal noise can be decreased by lowering the temperature and by employing a low dissipation (high Q) suspension, as seen from the expression for the effective thermal noise acceleration [16]

$$a_{\text{th}} = 2 \times 10^{-23} \left(\frac{T}{1\text{K}} \right)^{1/2} \left(\frac{1\text{day}}{\tau_0} \right)^{1/2} \left(\frac{10^6\text{s}}{\tau} \right)^{1/2} \left(\frac{10^{16}}{Q} \right)^{1/2} \frac{\text{cm}}{\text{s}^2}. \quad (5)$$

where τ is the measurement time, τ_0 is the oscillator period, and T is the operating temperature. A promising high- Q suspension method is a Meissner suspension consisting of a superconducting body floating above a superconducting coil. Niobium or NbTi in bulk or film form have been used in the past in such diverse applications as gravimeters [17], gyros [18], and gravitational wave antennas [19,20]. Generally the magnetic field applied to the superconductor is limited to $B \lesssim 0.2\text{T}$ to avoid flux penetration or loss of superconductivity [19,20]. However, even for small fields the magnetic flux exclusion is usually incomplete in polycrystalline Nb superconductors and flux creep will cause noise [21]. The lifting pressure $\propto B^2$ is limited to about 100 g/cm^2 . This could be dramatically increased by replacing the bulk superconductor with a persistent-mode superconducting magnet, as shown in Figure 2. Commonly used NbTi wire has a critical field of several T. Moreover, the flux lines are strongly pinned by artificial lattice defects in the magnet wire, leading to low levels of flux noise and dissipation. Very low resistance $\sim 10^{-14}\Omega$ [22] wire joints can be made by cold welding, and the magnetic field decay rate can be as low as $\dot{B}/B = R/L \sim 10^{-9}/\text{day}$, where R is the joint resistance and L is the inductance. The current decay due to losses in the joint will cause the suspended magnet to sink gradually. The concomitant change of magnetization will produce a slowly varying torque on the float due to the gyromagnetic (“Einstein-deHaas”) effect. Due to unavoidable deviations from cylindrical symmetry, the oscillator will have a very long, but finite rotational oscillation period. For small amplitudes, the oscillating supercurrents in the wire will cause the fluxoids to move elastically about their pinning centers, and very little dissipation is expected. In order to match the rotation period to the signal period ($\sim 1\text{ day}$), an additional restoring potential may be added. One possibility is a superconducting or low-loss dielectric (*e.g.* single-crystal sapphire) ellipsoid in the constant electric field of a parallel plate capacitor [16]. Both negative and positive torsion coefficients can be produced by aligning the long axis of the ellipsoid perpendicular or parallel to the field.

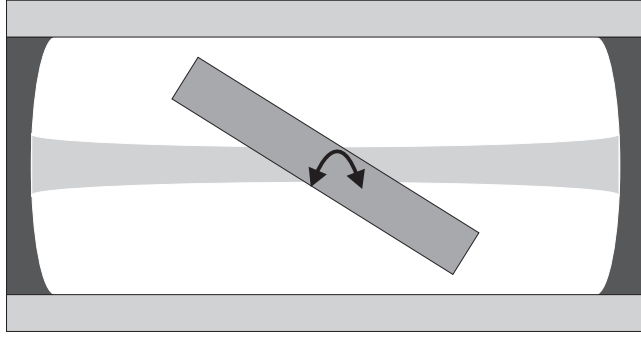


FIG. 3. Topview diagram of the high- Q tunable optical cavity. The cavity is operated in the TEM_{00p} Gaussian mode. A narrow linewidth $\sim 100\text{kHz}$ is achieved with high relectivity mirrors and a low-loss dielectric Brewster-angled plate. Two symmetrically placed and oppositely oriented fixed plates may be added to avoid transverse displacement of the beam.

The effects of time-varying gravity gradients can be reduced with a highly cylindrically symmetric target (see Figure 1). With the c.m. of the target centered below the suspension support, the leading order gravitational torque arise from the dipole moment of the torsion balance. For a source mass M at a distance R from the balance c.m., the torque is

$$\tau_z \simeq \frac{G_N M}{R^3} (I_x - I_y) \quad (6)$$

where I_x, I_y are the moments of inertia about the two horizontal axes. Diurnally varying mass distributions, *e.g.* changes of the atmospheric air mass due to solar heating, are especially worrisome. These effects can be minimized with a careful mechanical design and subsequent balancing steps using a movable laboratory source mass. In addition, locating the experiment in a deep mine would be beneficial. The gravitational interaction of the balance with the Sun and the Moon are less dangerous, because they produce torques with a 12 hr period to first order.

Low frequency seismic noise can also be a performance limiting factor in torsion balance experiments. At a period of ~ 24 hrs, the noise is dominated by tidal effects, with typical variations in the strain of $\Delta L/L \sim 10^{-7}$, in the tilt about the local (g-referenced) vertical axis of $\Delta\theta \sim 10^{-6}$ rad, and in the local gravitational acceleration of $\Delta g/g \sim 10^{-7}$. Small deviations from ideal symmetry will couple these motions into the rotational mode of the balance. For example, the tilt-rotation coupling of a tungsten fiber suspension is typically $\simeq 0.02$ [23]. Two possible remedies are (1) improving the symmetry of the balance, and (2) employing active anti-seismic isolation systems. A remaining worry is low frequency rotational seismic noise for which no reliable data is available. It will directly mask the signal and needs to be compensated.

The proposed angular rotation readout has very high immunity against vertical, horizontal, and tilt seismic noise. It consists of a parametric transducer, which converts the angle to an optical frequency. As shown in Figure 3, the transducer consists of a high- Q optical cavity of length l , tuned by a Brewster-angled low loss dielectric plate of thickness d . Using high-reflectivity mirrors and a cavity length ~ 10 cm should give linewidths of order 100 kHz for the Gaussian TEM_{00p} modes, with a frequency tuning sensitivity of $df/d\theta \sim f(d/l) \sim 10^{14}\text{Hz/rad}$. The angular measurement precision depends on the number of photons N via $\Delta\theta \sim \lambda/(dF\sqrt{N})$, where F is the cavity finesse, and λ is the laser wavelength. This is a factor $\sim F$ better than the optical lever readout for equal laser power. Cryogenic optical resonators have excellent long-term stability and have been proposed as secondary frequency standards. The measured frequency drifts range from $\sim 1\text{Hz}$ over minutes to $\sim 100\text{Hz}$ over days [24]. For the measurement of the rotation angle, a stable reference frequency will be required. This can be easily implemented using a laser locked to a second cavity. The described angle readout has little sensitivity to lateral, tilt, and vertical motion, but couples to rotational noise. A possible solution would be to suspend the target as well as the optical cavity in order to suppress the common rotation mode. The cavity suspension should have a much longer natural period than the

target suspension to avoid its excitation at the signal frequency. A different approach to suppress rotational noise would employ two identical torsion balances, but rotated by 180 degrees with respect to each other.

Additional background forces will arise from gas collisions, cosmic ray hits, radioactivity, solar neutrino and WIMP interactions resulting in a Brownian motion of the target. The equivalent acceleration is $a \sim (\bar{p}/m)\sqrt{n/\tau}$, where \bar{p} is the average momentum transfer, and n is the collision or decay rate. The requirements on the residual gas pressures are very severe with only a few collisions with the target allowed per second. Cryopumping and the use of getters will be essential. The cosmic muon flux at sea level is about $0.01 \text{ cm}^{-2} \text{ s}^{-1}$ with a mean energy of $\sim 1 \text{ GeV}$. Thus, a target of area 100 cm^2 will experience a collision rate $\sim \mathcal{O}(1) \text{ s}^{-1}$, causing an acceleration comparable to the signal in Equation 5. Cosmic rays can also lead to a net charge buildup of the torsion balance and spurious electrostatic forces. This background can be reduced by several orders of magnitude by going underground. Further disturbing forces may be caused by time-varying electric and magnetic background fields, which can be shielded with superconductors. Blackbody radiation and radiometric effects would be greatly reduced in a temperature controlled cryogenic environment.

Finally, there is a fundamental limit imposed by the uncertainty principle. The accuracy of a force measurement obtainable by continuously recording the test mass position (standard quantum limit) is

$$a_{\text{SQL}} = 5 \times 10^{-24} \left(\frac{10 \text{ kg}}{m} \right)^{1/2} \left(\frac{1 \text{ day}}{\tau_0} \right)^{1/2} \left(\frac{10^6 \text{ s}}{\tau} \right) \frac{\text{cm}}{\text{s}^2} \quad (7)$$

where m is the test mass, τ_0 is the oscillator period, and τ is the measurement time. In our proposed position readout, the disturbing back action force arises from spatial fluctuations in the photon flux passing through the central tuning plate. A laser beam pulse containing N photons, and centered on the plate rotation axis, will produce a random change in the angular momentum of the plate of $\Delta L \sim F\sqrt{N}\hbar\omega d/c$. Here, d is the average transverse photon displacement with respect to the rotation axis, which is also of order the plate thickness. A slightly higher sensitivity can be obtained with a stroboscopic “quantum nondemolition” (QND) measurement [25,26], where the test mass position is recorded every half period. Here,

$$a_{\text{QND}} = a_{\text{SQL}} \sqrt{\omega_0 \Delta t} \quad (8)$$

and Δt is the strobe duration.

There is hope that cosmic neutrinos will be detected in the laboratory early in the next century, especially if they have masses in the eV range and are of Dirac type. The most viable way seems to be a greatly improved torsion balance operated in a deep mine.

Naturally, the proposed torsion balance could also be applied to tests of the weak equivalence principle with the Sun as the source mass [27,28], and to searches for new short range ($\sim 1 \text{ m}$) forces with a movable laboratory mass [29,30,23].

ACKNOWLEDGMENTS

This research was performed by LLNL under the auspices of the U.S. Department of Energy under contract no. W-7405-ENG-48. I thank E. Adelberger, S. Baessler, I. Ferreras, A. Melissinos, R. Newman, P. Smith, and W. Stoeffl for useful discussions.

-
- [1] J. Primack, *Science* **280**, 1398 (1998); E. Gawiser and J. Silk, *Science* **280**, 1405 (1998).
 - [2] J. Primack and M. Gross, *astro-ph/9810204*.
 - [3] S. Tremaine and J.E. Gunn, *Phys. Rev. Lett.* **42**, 407 (1979)

- [4] J. Ellis and P. Sikivie, Phys. Lett. **B321**, 390 (1994).
- [5] L. Stodolsky, Phys. Rev. Lett. **34**, 110 (1974).
- [6] R. Opher, Astron. Astrophys. **37**, 135 (1974).
- [7] R. Lewis, Phys. Rev. **D21**, 663 (1980).
- [8] R. Opher, Astron. Astrophys. **108**, 1 (1982).
- [9] N. Cabibbo and L. Maiani, Phys. Lett. **B114**, 115 (1982).
- [10] P. Langacker, J.P. Leveille, and J. Sheiman, Phys. Rev. **D27**, 1228 (1983).
- [11] V.F. Shvartsman, V.B. Braginski, S.S. Gershtein, Y.B. Zel'dovich, and M.Y. Khlopov, JETP Lett. **36**, 277 (1982).
- [12] P.F. Smith and J.D. Lewin, Phys. Lett. **B127**, 185 (1983); Acta Phys. Polon. **B15**, 1201 (1984); Acta Phys. Polon. **B16**, 837 (1985); Astrophys. J. **318**, 738 (1987); P.F. Smith, Nuovo Cimento **83A**, 263 (1984); J.D. Lewin and P.F. Smith, Astrophys. Lett. **24**, 59 (1984); P.F. Smith and J.D. Lewin, Phys. Rep. **187**, 203 (1990).
- [13] I. Ferreras and I. Wasserman, Phys. Rev. **D52**, 5459 (1995).
- [14] C.C. Speake and J. Leon, Class. Quantum Grav. **13**, A207 (1996).
- [15] E. Adelberger, private communication.
- [16] V. Braginsky and A. Manukin, Measurements of Weak Forces in Physics Experiments, (The University of Chicago Press, Chicago, 1977).
- [17] W. Prothero and J. Goodkind, Rev. Sci. Instrum. **39**, 1257 (1968).
- [18] J. Harding and R. Tuffias, Adv. Cryog. Eng. **6**, 95 (1961).
- [19] S. Boughn, W. Fairbank, R. Giffard, J. Hollenhorst, M. McAshan, H. Park, and R. Taber, Phys. Rev. Lett. **38** 454 (1977).
- [20] D. Blair, M. Buckingham, C. Edwards, J. Ferreirinho, D. Howe, R. James, F. van Kann, and A. Mann, J. de Physique **40**, L112 (1979).
- [21] P. Karen, G. Gillies, and R. Ritter, Rev. Sci. Instrum. **61**, 1494 (1990).
- [22] M. Leupold and Y. Iwasa, Cryogenics **16**, 215 (1976).
- [23] Y. Su, B. Heckel, E. Adelberger, J. Gundlach, M. Harris, G. Smith, and H. Swanson, Phys. Rev. **D50**, 3614 (1994).
- [24] S. Seel, R. Storz, G. Ruoso, J. Mlynek, and S. Schiller, Phys. Rev. Lett. **78**, 4741 (1997); R. Storz, C. Braxmaier, K. Jäck, O. Pradl, and S. Schiller, Opt. Lett. **23**, 1031 (1998).
- [25] V. Braginsky, Y. Vorontsov, and K. Thorne, Science **209**, 547 (1980).
- [26] V. Braginsky and F. Khalili, Quantum Measurement, (Cambridge University Press, Cambridge, 1992).
- [27] P. Roll, R. Krotkov, and R. Dicke, Ann. Phys. (N.Y.) **26**, 442 (1964).
- [28] V. Braginsky and V. Panov, JETP Lett. **34**, 463 (1972).
- [29] J. Moody and F. Wilczek, Phys. Rev. **D30**, 130 (1984).
- [30] E. Adelberger, B. Heckel, C. Stubbs, and W. Rogers, Annu. Rev. Nucl. Part. Sci. **41**, 269 (1991).